



**Fermi National Accelerator Laboratory**

**FERMILAB Conf-96/336-E  
DØ**

## **DØ Top Quark Mass Analysis**

**M. Strovink**

**For the DØ Collaboration**

*Physics Department and Lawrence Berkeley National Laboratory  
University of California, Berkeley, California 94720*

*Fermi National Accelerator Laboratory  
P.O. Box 500, Batavia, Illinois 60506-0500*

October 1996

Published Proceedings of the *XI Topical Workshop on  $\bar{p}p$  Collider Physics*, Abano Terme (Padova), Italy,  
May 27-June 1, 1996.

## **Disclaimer**

*This report was prepared as an account of work sponsored by an agency of the United States Government. Neither the United States Government nor any agency thereof, nor any of their employees, makes any warranty, express or implied, or assumes any legal liability or responsibility for the accuracy, completeness or usefulness of any information, apparatus, product or process disclosed, or represents that its use would not infringe privately owned rights. Reference herein to any specific commercial product, process or service by trade name, trademark, manufacturer or otherwise, does not necessarily constitute or imply its endorsement, recommendation or favoring by the United States Government or any agency thereof. The views and opinions of authors expressed herein do not necessarily state or reflect those of the United States Government or any agency thereof.*

## **Distribution**

*Approved for public release: further dissemination unlimited.*

# DØ TOP QUARK MASS ANALYSIS

M. STROVINK for the DØ Collaboration

*Physics Department and Lawrence Berkeley National Laboratory,  
University of California, Berkeley, CA 94720, USA*

—  
*Fermi National Accelerator Laboratory, Batavia, IL 60510, USA*

I report on DØ's preliminary analyses of the top quark mass  $m_t$  based on an exposure at  $\sqrt{s} = 1.8$  TeV with integrated luminosity  $\approx 100 \text{ pb}^{-1}$  at the Fermilab Tevatron  $p\bar{p}$  collider. From three  $e + \mu + \geq 2$  jet events (with background  $0.36 \pm 0.09$ ), using partly original methods, we obtain  $m_t = 158 \pm 24(\text{stat}) \pm 10(\text{syst}) \text{ GeV}/c^2$ . From 30  $e$  or  $\mu + \geq 4$  jets events (with background  $17.4 \pm 2.2$ ), we find  $m_t = 170 \pm 15(\text{stat}) \pm 10(\text{syst}) \text{ GeV}/c^2$ . Recently, using multivariate methods based on particular kinematic variables, we have learned how to improve the background suppression in the latter sample without unduly distorting the reconstructed top mass spectra. Applying these methods should improve considerably the accuracy of our top quark mass determination.

## 1 Introduction

In the initial observations<sup>1</sup> of the top quark, analyses of its mass in the lepton +  $\geq 4$  jets channel were essential ingredients. And in an early publication<sup>2</sup>, for one  $e + \mu + 2$  jet event having low background probability, DØ described briefly a top quark mass analysis carried out in the dilepton channel. More recently we have done much additional work in both channels.

Most of this report is devoted to results first made public<sup>3</sup> in March 1996. In the dilepton channel, where the top mass accuracy is limited primarily by statistics, the analysis and result have remained essentially unchanged since that time. I aim to motivate and explain this analysis. In the lepton + jets channel, work continues at a furious pace. Very recent progress in background suppression has not yet propagated into a new top quark mass result. For that reason I describe only briefly DØ's March 1996 result in this channel, concluding with a short account of the new advance in analysis technique. All figures and results in this report remain preliminary.

## 2 Top Quark Mass from Events with Two Isolated Leptons

Given the top quark mass  $m_t$  and neglecting jet masses, the process

$$p + \bar{p} \rightarrow t + \bar{t} + X$$

$$\begin{aligned}
t &\rightarrow W^+ + b_{\text{jet1}} & W^+ &\rightarrow e^+ + \nu_e \\
\bar{t} &\rightarrow W^- + \bar{b}_{\text{jet2}} & W^- &\rightarrow \mu^- + \bar{\nu}_\mu
\end{aligned}$$

is 0C with 14 observables, *e.g.*  $\{o_1 \dots o_{14}\} \equiv \{\mathbf{p}(e, \mu, \text{jet1}, \text{jet2}), \mathbf{p}_\perp(t\bar{t})\}$ . The 0C fit solves a quartic equation equivalent to the geometrical construction of Dalitz, Goldstein and Kondo<sup>4</sup>, usually yielding two or four solutions over a wide range of  $m_t$ . We narrow this range by weighting the solutions.

### 2.1 Weighting the Top Quark Mass Solutions

In the high resolution limit, the general weight is

$$w(m_t) = \frac{d^{14}\sigma(t\bar{t})}{\sigma_{\text{vis}}(t\bar{t}) d o_1 \dots d o_{14}} ,$$

where “ $\sigma$ ” reflects the decay as well as the production matrix elements. For any event with a fixed jet assignment,  $w$  is invariant to the choice of observables  $\{o_i\}$ . The visible cross section divisor  $\sigma_{\text{vis}}(t\bar{t})$  removes the *a priori* bias favoring low  $m_t$ . To compute  $d\sigma(t\bar{t})/d\{o_i\}$ , one multiplies the readily calculable  $d\sigma(t\bar{t})/d\text{LIPS}$  by the Jacobian factor  $J = |\frac{\partial \text{LIPS}}{\partial \{o_i\}}|$ . This factor favors solutions for which a large Lorentz invariant phase space volume maps into a small observable phase space volume. Typically, for a given set of observables,  $J$  varies widely with  $m_t$ . This same general weight was used in one analysis<sup>5</sup> of DØ’s first low background top-to-dilepton candidate.

For high-statistics Monte Carlo (MC) tests,  $w$  is cumbersome to compute. Simplifying it does not grossly degrade the mass resolution, which is dominated by other effects such as measurement error, jet combinatorics, and gluon radiation. At present DØ uses two methods with independent simplified weights. Data and MC are always treated symmetrically, so both methods are unbiased. They turn out to be comparably efficient as well.

Following Dalitz and Goldstein, Method 1’s weight neglects the Jacobian and substitutes the parton-density-function product  $q\bar{q}$  for the  $t\bar{t}$  production piece of  $d\sigma(t\bar{t})/d\text{LIPS}$ . We use the weight

$$w_1(m_t) = A(m_t) q(x) \bar{q}(\bar{x}) P(E_e^{\text{CM of } t}) P(E_\mu^{\text{CM of } \bar{t}}) ,$$

where the  $P$ ’s are decay probability densities. We extend Dalitz and Goldstein’s technique by introducing  $A(m_t)$ , a function chosen empirically to cancel the  $m_t$  bias, and by fitting the measured rather than an assumed value of  $\mathbf{p}_\perp(t\bar{t})$ . An early application of Method 1 also has been described<sup>5</sup>.

Method 2's weight is the complement of Method 1's. Here we neglect the production and decay factors in favor of a “neutrino phase space” approximation to the Jacobian. Fixing the measured jet and lepton momenta, we step the two neutrinos through their expected distributions in  $\eta$ . Each pair  $\eta_m \eta_n$  yields a 0C fit, which is given a weight  $w_{mn}$  based on compatibility between fit and measured missing  $E_T$  (which is not used by the fit). The weight  $w_2(m_t)$  is the sum of the  $w_{mn}$ 's. We find that the product  $w_2 w_1$  is not significantly more efficient than  $w_2$ , so we choose to keep the two weights complementary.

## 2.2 Common Aspects of Methods 1 and 2

Weights aside, Methods 1 and 2 share several features. Because we are not in the high resolution limit, for both methods we smear the measured parameters of each event many times within the experimental resolution and sum the weights from each smear to get  $w(m_t)$  for that event. After summing the weights for the two different jet-lepton pairings and the 0, 2, or 4 different solutions per pairing, we take the  $m_t$  which maximizes this summed weight to be the single reconstructed top mass  $m_{\text{fitted}}$  for each event. If a third jet is present, (A) we assume that it is initial state gluon radiation (ISR), or (B) we assign a probability to the hypothesis that it is final state radiation (FSR), to be included in  $m_{\text{fitted}}$ . For events in which  $m_{\text{fitted}}^A$  is quite different from  $m_{\text{fitted}}^B$ , MC experiments show that it helps to average the two, which we do.

## 2.3 Event Selection, Event Likelihoods, and Mass Resolution Functions

In the dilepton channel, event selection is the same as in  $D\bar{O}$ 's top cross section analysis described elsewhere<sup>6</sup> in these Proceedings. Three  $e + \mu + 2$  jet events are observed, *vs.* a calculated background of  $0.36 \pm 0.09$ . One additional event is found in each of the  $e e j j$  and  $\mu \mu j j$  channels; the background for all three channels is  $1.6 \pm 0.4$  events. Figure 1 displays Method 2's weight  $w_2$  *vs.*  $m_t$  for all five events. Contours labeled 2j (3j) use the just described procedure A (B) for three jet events. Method 1's weight  $w_1$  is similarly distributed.

Figure 2 displays the distribution of top quark mass reconstructed by Method 2 for background and for five values of MC top quark mass. The peaks of these distributions track the generated mass with a small departure from linearity. Method 1's top quark mass resolution functions are similar.

## 2.4 Common Features of Dilepton and Lepton + Jets Top Mass Analyses

Mass reconstruction methods aside, the dilepton and lepton + jets top quark mass analyses share common methods. For both analyses we construct templates

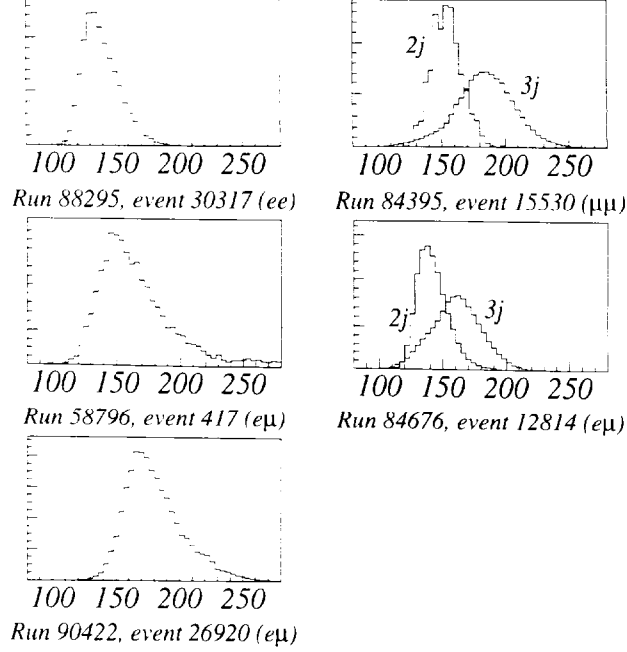


Figure 1: Method 2 weight  $w_2$  (see text) vs. top mass for five dilepton candidates. Curves “2j” (“3j”) apply procedure A (B) (see text) for three jet events.

in  $m_t$  for backgrounds and various top masses, such as those in Fig. 2. We make maximum likelihood fits to  $m_t$  and the expected number  $\langle n_s \rangle$  of signal and  $\langle n_b \rangle$  of background events in the sample, using the external constraint on  $\langle n_b \rangle$  (with errors) provided by the counting experiment. We base quoted statistical errors not on the likelihood curves, but rather on studies of ensembles of MC experiments (“ensemble tests”) in which  $n_s$  and  $n_b$  as well as the event kinematics are allowed to fluctuate. This tends to increase the errors.

An example of these ensemble tests, drawn from the Method 1 dilepton analysis, is exhibited in Fig. 3 for a generated top quark mass of  $150 \text{ GeV}/c^2$ . At masses where sets of MC top events exist, we evaluate  $\ln \mathcal{L}$ , where  $\mathcal{L}$  is the maximum likelihood from a fit to a mixture of background and top. To the five mass points yielding the largest  $\ln \mathcal{L}$  a parabola is fit, whose peak  $m_{\text{fit}}$  is taken to be the best fit top quark mass. Plotted is the distribution of  $m_{\text{fit}}$  for a large ensemble of MC experiments. The statistical error is defined by the smallest interval which contains 68% of the entries.

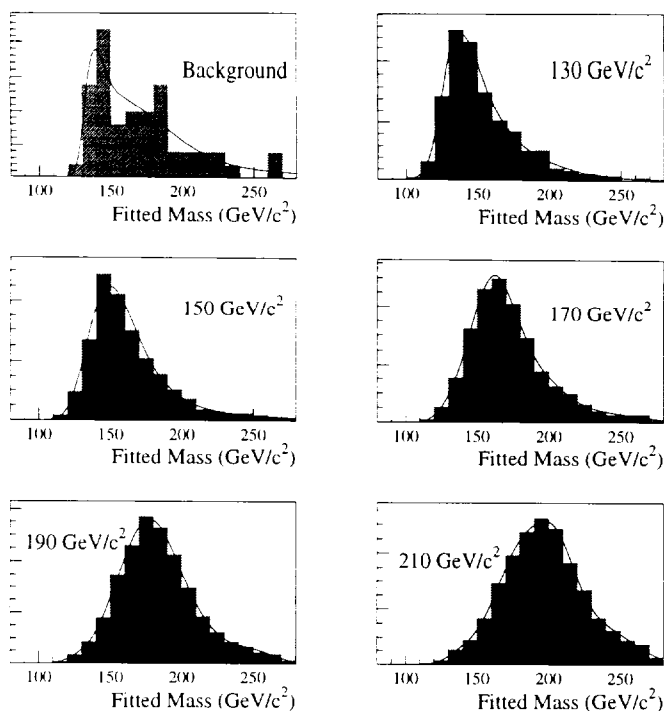


Figure 2: MC events per  $10 \text{ GeV}/c^2$  vs.  $m_{\text{fitted}}$  from Method 2, for background and for five top quark masses.

## 2.5 Dilepton Top Quark Mass Results

Figure 4 shows the results of the Method 2 analysis, for (a) the  $e\mu$  channel, and (b) all three dilepton channels combined. The smooth curves display the parametrized resolution templates for background, top with best fit mass, and best fit top and background mixture. The results are (a)  $m_t = 157 \pm 23(\text{stat}) \pm 9(\text{syst})$  and (b)  $m_t = 157^{+20}_{-32}(\text{stat}) \pm 9(\text{syst}) \text{ GeV}/c^2$ . Note that the statistical error on result (a) would be  $\approx 35\%$  smaller if it were determined from the likelihood curve rather than the ensemble tests.

Correspondingly, the Method 1 results are exhibited in Fig. 5. In this method the resolution templates are used (and displayed) in unparametrized form. For all three dilepton channels combined, the result is  $m_t = 151 \pm 21(\text{stat}) \pm 10(\text{syst}) \text{ GeV}/c^2$ , and, for the  $e\mu$  channel alone,

$$m_t = 158 \pm 24(\text{stat}) \pm 10(\text{syst}) \text{ GeV}/c^2.$$

DØ quotes this last result, using Method 1 because it is more mature, and emphasizing the  $e\mu$  channel because it has especially low background.

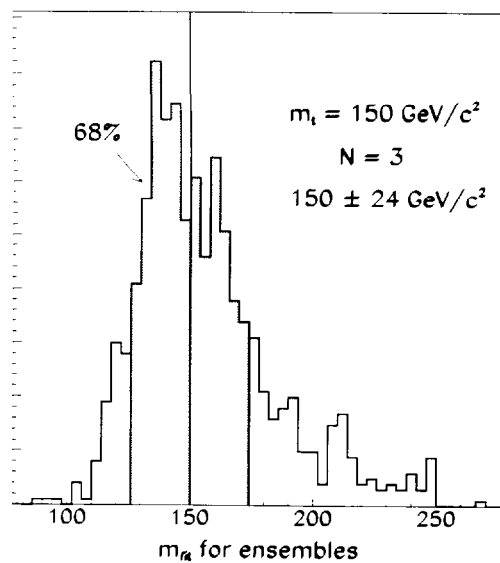


Figure 3: Entries per  $4 \text{ GeV}/c^2$  vs. Method 1 best fit top quark mass  $m_{\text{fit}}$  for an ensemble of MC experiments having 3  $e\mu$  events and, on average, the expected mixture of  $150 \text{ GeV}/c^2$  top and background events. 68% of the experiments yield a result within  $24 \text{ GeV}/c^2$  of the generated mass.

The systematic errors listed above are the sums in quadrature of the effects of uncertainties due to jet energy scale ( $\pm 5 \text{ GeV}/c^2$ ), variation of the top quark event generator ( $\pm 5 \text{ GeV}/c^2$ ), MC statistics ( $\pm 5 \text{ GeV}/c^2$ ), and shape of the background templates in  $m_{\text{fitted}}$  ( $\pm 4 \text{ GeV}/c^2$ ). These uncertainties are for Method 1; they are essentially the same for Method 2. I return below to the jet energy scale.

### 3 Top Quark Mass from Events with One Isolated Lepton

#### 3.1 Reconstructing the Top Quark Mass: Combinatorics

With one neutrino unmeasured rather than two, fits to lepton + jets final states are 2C (with  $m_t$  fit) rather than 0C (with  $m_t$  assumed) in the dilepton case. The two constraints are

$$\begin{aligned} m(b_{\text{jet1}}W(\rightarrow l\nu)) &= m(b_{\text{jet2}}W(\rightarrow \text{jet3jet4})) \\ m(W(\rightarrow \text{jet3jet4})) &= m_{\text{pole}}^W. \end{aligned}$$

We do not measure  $p_z(\nu)$ ; it is determined by the requirement  $m(W(\rightarrow l\nu)) = m_{\text{pole}}^W$ . Among the lepton + jets mass fitting routines in use by DØ, three minimize the  $\chi^2$  constructed from the inverse measurement-error matrix; one (used

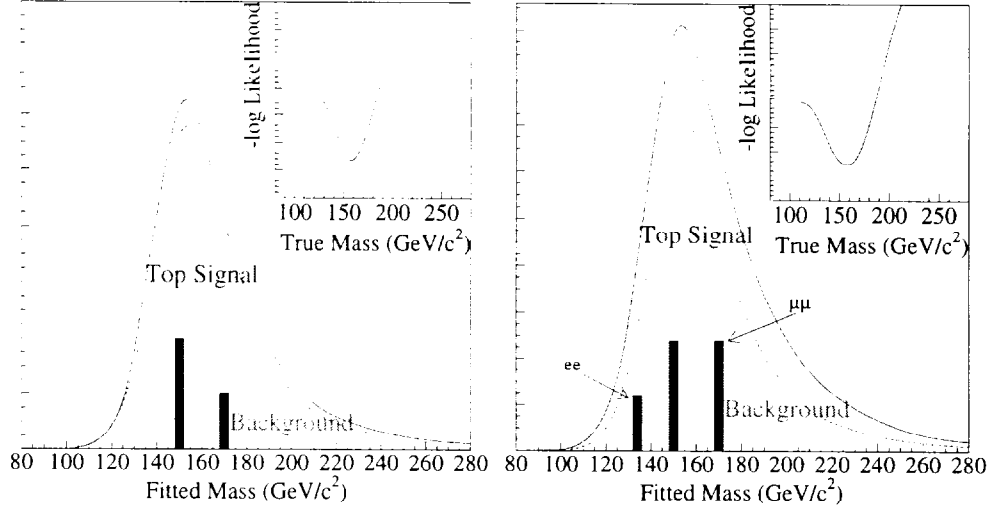


Figure 4: Method 2 results (a) for the  $e\mu$  and (b) for all three dilepton channels. The dashed (dotted) curves are the distributions in  $m_{\text{fitted}}$  expected for best fit top signal (background), and the solid curve is their sum. Boxes show the candidate events. Inset is  $-\ln \mathcal{L}$  (unit increment per division) vs.  $m_t$ .

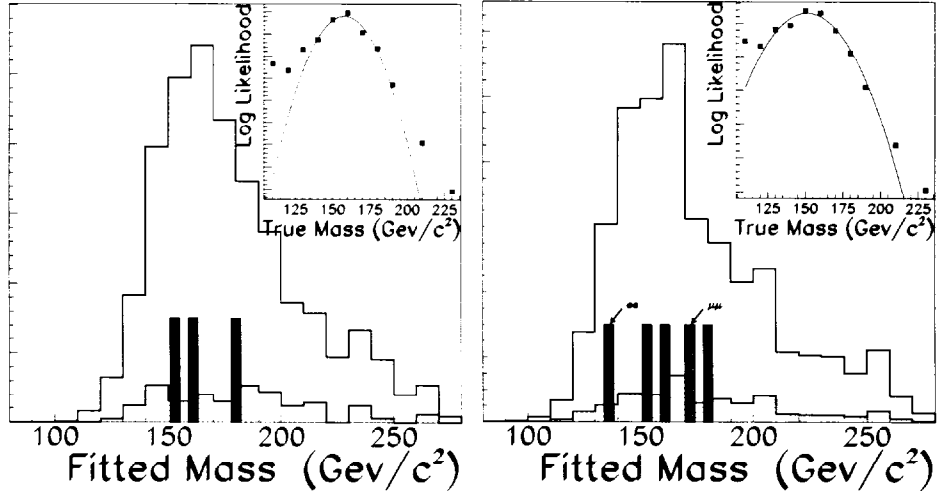


Figure 5: Method 1 results (a) for the  $e\mu$  and (b) for all three dilepton channels. White (shaded) histograms are arbitrarily normalized distributions in  $m_{\text{fitted}}$  expected for best fit top (background); dark boxes show the candidate events. Shown in the inset are values of  $\ln \mathcal{L}$  (unit increment per division) vs.  $m_t$ , with a quadratic fit to the five highest points.

for work described in Sec. 4) minimizes a  $\chi^2$  based on the above constraint equations.

There are 12 possible jet assignments (6 for events in which a soft muon

tags a  $b$  quark). Usually the fitted top quark mass  $m_{\text{fitted}}$  varies strongly with reassignment of  $b_{\text{jet1}}$  (4 permutations), and less strongly with reassignment of  $b_{\text{jet2}}$  when  $b_{\text{jet1}}$  is fixed (3 permutations or 1). Also, with the jet assignment fixed, often there are local  $\chi^2$  minima for each of two solutions for  $p_z(\nu)$ . Minimizing  $\chi^2$  does yield the best fit to a fixed permutation, but for typical measuring errors the lowest  $\chi^2$  permutation often is not correct. Also, ISR and FSR frequently cause the four highest  $E_T$  jets not to correspond to the four quarks to which one wishes to fit. These combinatoric uncertainties make necessary, as in the dilepton case, a statistical determination of  $m_t$  in which the relationship between true and fitted top quark mass varies in a complex way from event to event.

### 3.2 Jet Energy Calibration and Event Selection

Both the dilepton and lepton + jets top quark mass analyses use jets clustered within a cone of half-angle  $\Delta\mathcal{R} = 0.5$  in  $\eta$ - $\phi$  space. The jet energies are calibrated *in situ* by standard DØ methods<sup>8</sup> which impose transverse energy balance in  $\gamma$  + jet events; the electromagnetic energy calibration in turn is fixed by reconstructing  $Z^0 \rightarrow e\bar{e}$  decays. For the lepton + jets analysis, additional parton-out-of-cone (OOC) corrections based on HERWIG simulated top MC events slightly inflate the reconstructed jet energies to represent those of the primary partons. Because exactly the same OOC corrections are applied both to data and top MC, to lowest order they do not shift the top quark mass result. They do improve the accuracy of the constrained fit. We check the jet energy calibration by testing the transverse energy balance in reconstructed  $Z(\rightarrow e\bar{e})$  + jet final states. On that basis we assign a systematic error of  $\pm(4\% + 1 \text{ GeV})$  to the jet energy scale.

Lepton + jets events are selected for mass analysis in the same way described elsewhere in these Proceedings<sup>7</sup> for DØ's counting experiment, with a few exceptions. For events without soft muon tags, the cuts on  $H_T$  and aplanarity are dropped in favor of the requirements  $|\eta_W| < 2$  and  $\mathcal{D}_{\text{early}} > 0.55$ , where  $\mathcal{D}_{\text{early}}$  is an early version of the top likelihood discriminant described in Sec. 4.1. For tagged events, the (weaker) cuts on  $H_T$  and aplanarity are dropped in favor of requiring a fourth jet passing the same jet cuts  $E_T > 15 \text{ GeV}$  and  $|\eta| < 2$  which are imposed in other DØ top analyses. Finally, all events must survive a 2C kinematic fit (as described in Sec. 3.1) with  $\chi^2 < 7$ .

### 3.3 Top Quark Mass Spectrum and Result

In other respects, our method for top quark mass analysis in the lepton + jets channel closely follows that described<sup>1,9</sup> one year ago. We obtain the fitted mass

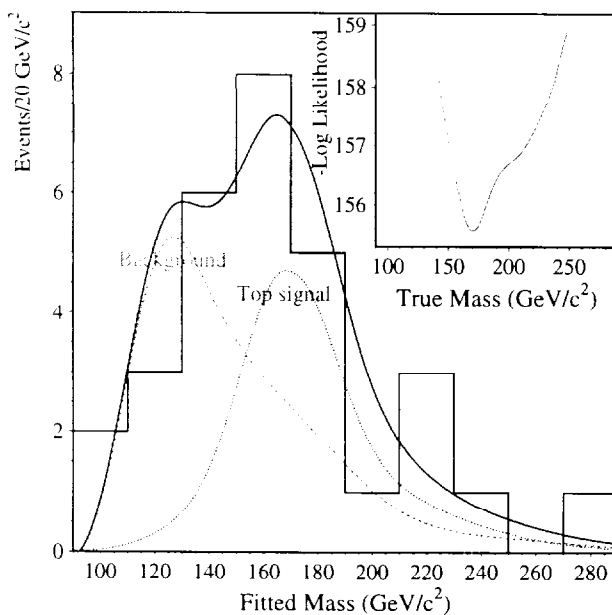


Figure 6: Result for the lepton + jets channel. The dotted (dashed) curves are the distributions in  $m_{\text{fitted}}$  expected for best fit top signal (background), and the solid curve is their sum. Inset is  $-\ln \mathcal{L}$  vs.  $m_t$ .

spectrum shown in Fig. 6 for 30 events passing cuts. The result of a maximum likelihood fit of the type described in Sec. 2.4, with  $\langle n_b \rangle$  constrained to  $17.4 \pm 2.2$  events from the counting experiment, is

$$m_t = 170 \pm 15(\text{stat}) \pm 10(\text{syst}) \text{ GeV}/c^2.$$

The three smooth curves in Fig. 6 show the background and the top signal corresponding to this best fit, and their sum.

The quoted statistical error is based on 1000 MC experiments of 30 events each in which  $m_t = 170 \text{ GeV}/c^2$  and the expected background is 17.4 events. A gaussian fit to the  $m_t$  distribution has a mean of 169.8 and an rms of 15.0  $\text{GeV}/c^2$ . If instead it were assigned using the likelihood curve depicted in the inset to Fig. 6, the statistical error would be smaller.

Other ensemble tests are used to propagate the systematic uncertainties to a top quark mass error. The  $\pm(4\% + 1 \text{ GeV})$  energy scale uncertainty mentioned in Sec. 3.2 propagates to  $\pm 7 \text{ GeV}/c^2$ . A  $\pm 6 \text{ GeV}/c^2$  error in  $m_t$  arises from variations among MC generators and jet definitions;  $\pm 3 \text{ GeV}/c^2$  from variations in background shape;  $\pm 3 \text{ GeV}/c^2$  from changes in maximum likelihood fitting method; and  $\pm 1 \text{ GeV}/c^2$  from MC statistics. Their sum in quadrature is 10  $\text{GeV}/c^2$ .

## 4 Progress in Analysis Methods for the Lepton + $\geq 4$ Jet Channel

Our present  $\pm 15$  GeV/ $c^2$  statistical error on the top quark mass in the lepton + jets channel is sensitive to the level of background, which we seek both to reduce and to assess more accurately. Our path to both goals exploits a particular set of kinematic variables, which are used to define a top likelihood discriminant  $\mathcal{D}$ .

### 4.1 Top Likelihood Discriminant

To construct  $\mathcal{D}$ , we first identify kinematic variables which discriminate top from background with similar reconstructed top mass, without significantly biasing the spectrum in  $m_{\text{fitted}}$  of either top or background. We use

$$\begin{aligned} \text{missing } E_T & \quad (\text{distribution in vicinity of lower bound}) \\ \text{aplanarity} & \propto \text{least eigenvalue of } \mathcal{P} \text{ tensor} \\ H'_{T2} & \equiv \frac{H_T - E_T^{j1}}{H_{\parallel}} \\ K'_{T\min} & \equiv \frac{(\min \text{ of } 6 \Delta \mathcal{R}_{jj}) \cdot E_T^{\text{lesser } j}}{E_T^W}. \end{aligned}$$

Here  $H_T$  is the scalar  $E_T$  of the jets,  $E_T^W$  is the scalar  $E_T$  of the leptons, and  $H_{\parallel}$  is the scalar  $|p_z|$  of the jets and leptons. For the cut on  $\mathcal{D}_{\text{early}}$  described in Sec. 3.2, we used in place of the last two variables

$$h \equiv \frac{E_T^W}{H_T + p_T^W} \quad \eta_{\text{rms}} \equiv \sqrt{\frac{\sum_{\text{jets}+W} E_T^i \eta_i^2}{\sum_{\text{jets}+W} E_T^i}}.$$

Distributions of top and background *vs.* functions of the last three variables, which largely determine  $\mathcal{D}$ , are exhibited in Fig. 7 (a-c). For events in these distributions,  $m_{\text{fitted}}$  is required to exceed 150 GeV/ $c^2$ , so that signal and background have the same average  $m_{\text{fitted}}$ . Although some discrimination is available from each variable, there is no obvious place to cut; a multivariate technique is needed.

To form  $\mathcal{D}$ , for distributions in each variable  $v_i$  we parametrize the normalized ratio of top to background  $\ln \mathcal{L}_i(v_i)$ . For each event we construct  $\ln \mathcal{L} \equiv \sum_i \omega_i \ln \mathcal{L}_i$ , where  $\omega_i$  is a constant weight. Taking into account the correlations of the  $\ln \mathcal{L}_i$  with  $m_{\text{fitted}}$  and with each other, we choose the  $\omega_i$  to optimize the signal-to-noise while requiring a null correlation of  $\ln \mathcal{L}$  with  $m_{\text{fitted}}$ . Finally we take  $\mathcal{D} \equiv \mathcal{L}/(1 + \mathcal{L})$ . Figure 7 (d), without any requirement on  $m_{\text{fitted}}$ , exhibits the distribution of  $\mathcal{D}$  for top and background. We require  $\mathcal{D} > 0.43$ , based

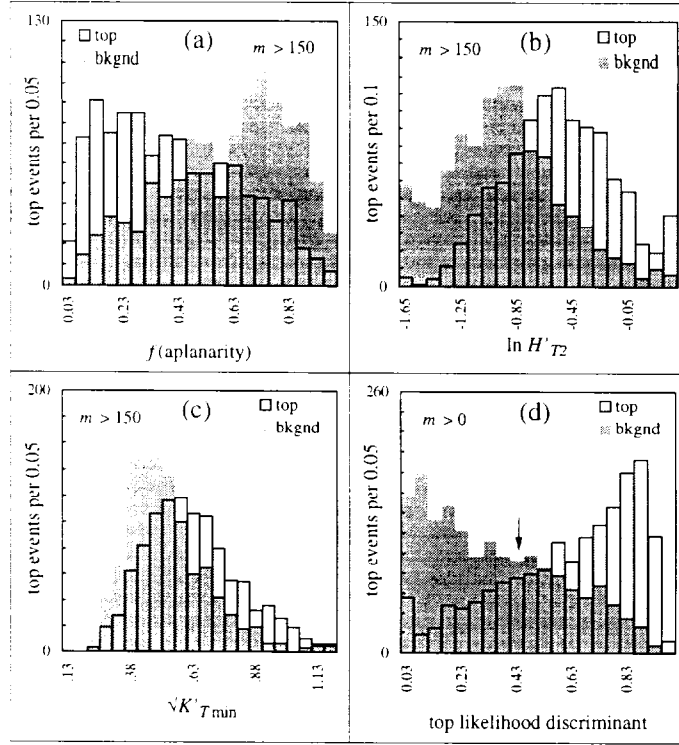


Figure 7: Distributions of MC top (light) and background (dark) lepton + jets events *vs.* functions of (a) aplanarity, (b)  $H'_{T2}$ , and (c)  $K'_{Tmin}$  for  $m_{\text{fitted}} > 150 \text{ GeV}/c^2$ , and (d) *vs.* top likelihood discriminant  $\mathcal{D}$  for all  $m_{\text{fitted}}$ ; the arrow shows the cut. Pairs of histograms are normalized to equal area.

on MC optimizations of the expected overall error on top quark mass. We also apply a light cut on  $H_{T2} \equiv H_T - E_T^{j1}$  to control the shape of the background spectrum at very low  $m_{\text{fitted}}$ . Neural networks trained on the same variables provide similar discrimination.

#### 4.2 Expectations for Use of Top Likelihood Discriminant

Figure 8 exhibits the distributions in  $m_{\text{fitted}}$  for background and for MC top events with generated masses of 160, 180, and 200  $\text{GeV}/c^2$ , after the cuts  $\mathcal{D} > 0.43$  and  $H_{T2} > 70 \text{ GeV}$  are applied. The peaks of the top distributions still track the generated mass, with no measurable loss of linearity as a result of the cut, and the background continues to peak much lower, falling monotonically in the region of the top mass peak. Figure 9 summarizes the effect of a combined  $\mathcal{D} > 0.43$  and  $H_{T2} > 90 \text{ GeV}$  cut, applied only to untagged events, for a typical mixture of MC top and background including tagged events. These cuts retain more than  $\frac{3}{4}$

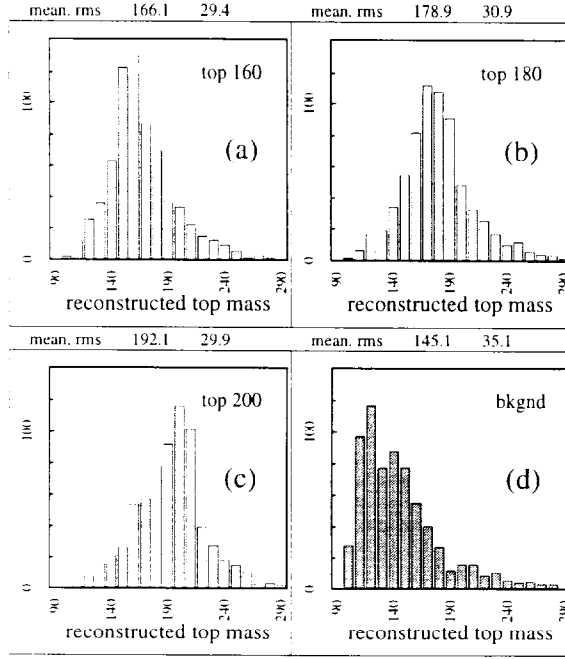


Figure 8: Distributions of MC (a) top 160, (b) top 180, (c) top 200, and (d) background events, normalized to the same area, *vs.*  $m_{\text{fitted}}$  after the cuts  $\mathcal{D} > 0.43$  and  $H_{T2} > 70 \text{ GeV}/c^2$ .

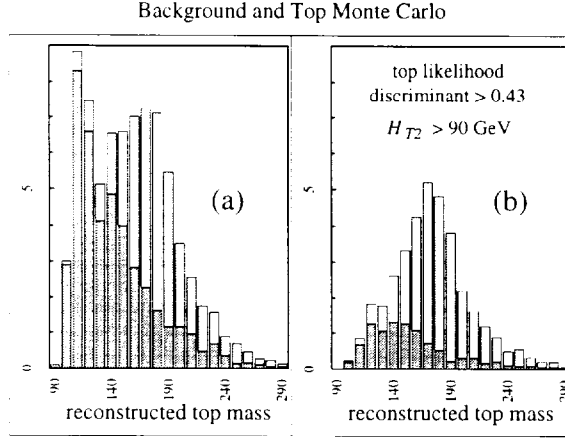


Figure 9: Distributions *vs.*  $m_{\text{fitted}}$  for a typical mixture of  $180 \text{ GeV}/c^2$  MC top + background (light) and background (dark) events, including tags, (a) before and (b) after the cuts  $\mathcal{D} > 0.43$  and  $H_{T2} > 90 \text{ GeV}/c^2$  are applied to untagged events only.

of the signal, but less than  $\frac{1}{4}$  of the background. Comparing the signal-to-noise in Fig. 9 (b) to that in Fig. 6, we expect to achieve a substantial improvement in top quark mass accuracy in the lepton + jets channel<sup>10</sup>.

## Acknowledgements

We thank the staffs at Fermilab and the collaborating institutions for their contributions to the success of this work, and acknowledge support from the Department of Energy and National Science Foundation (U.S.A.), Commissariat à L'Energie Atomique (France), Ministries for Atomic Energy and Science and Technology Policy (Russia), CNPq (Brazil), Departments of Atomic Energy and Science and Education (India), Colciencias (Colombia), CONACyT (Mexico), Ministry of Education and KOSEF (Korea), CONICET and UBACyT (Argentina), and the A.P. Sloan Foundation.

## References

1. CDF Collaboration. F. Abe *et al.*, *Phys. Rev. Lett.* **74**, 2626 (1995); DØ Collaboration. S. Abachi *et al.*, *Phys. Rev. Lett.* **74**, 2632 (1995).
2. DØ Collaboration. S. Abachi *et al.*, *Phys. Rev. Lett.* **72**, 2138 (1994).
3. DØ Collaboration. M. Narain, to be published in *Proceedings, Les Rencontres de Physique de la Vallée d'Aoste*, La Thuile (1996), FERMILAB CONF-96/192-E; DØ Collaboration. R. Partridge, to be published in *Proceedings of the XXXI<sup>st</sup> Rencontres de Moriond*, Les Arcs, France (1996).
4. R.H. Dalitz and G.R. Goldstein, *Phys. Lett. B* **287**, 225 (1992); K. Kondo, T. Chikamatsu, and S. Kim, *J. Phys. Soc. Jpn.* **62**, 1177 (1993).
5. DØ Collaboration. M. Strovink, in *Proceedings of the International Europhysics Conference on High Energy Physics*, Marseille (1993), eds. J. Carr and M. Perrottet (Editions Frontieres, France, 1994), 292-296.
6. DØ Collaboration. D. Chakraborty, these Proceedings.
7. DØ Collaboration. John Butler, these Proceedings.
8. DØ Collaboration. R. Kehoe, to be published in *Proc. 6<sup>th</sup> Int. Conf. on Calorimeters in High Energy Phys.*, Frascati (1996).
9. DØ Collaboration. M. Strovink, in *Proceedings of the 10<sup>th</sup> Topical Workshop on Proton-Antiproton Collider Physics*, Batavia, IL (1995), eds. R. Raja and J. Yoh (American Institute of Physics, 1996), 320-337; DØ Collaboration. S. Snyder, in *Proceedings of the International Europhysics Conference on High Energy Physics*, Brussels, ed. J. Lemmone *et al.* (World Scientific, 1995), 655.
10. DØ Collaboration. S. Protopopescu, to be published in *Proceedings, International Conference on High Energy Physics*, Warsaw (1996). Quoted therein is the preliminary result  $m_t = 169 \pm 8(\text{stat}) \pm 8(\text{syst}) \text{ GeV}/c^2$ , based on the same event selection criteria used for Fig. 9 (b) in this report.